The Raman spectrum of $CaCO_3$ polymorphs calcite and aragonite. A combined experimental and computational study

Marco De La Pierre,[1] Cédric Carteret,[2] Lorenzo Maschio,[1]
Erwan André,[2] Roberto Orlando,[1] and Roberto Dovesi[1]

[1]*Dipartimento di Chimica, Università di Torino and NIS (Nanostructured Interfaces and Surfaces) Centre of Excellence, Via P. Giuria 7, 10125 Torino, Italy*

[2]*Laboratoire de Chimie Physique et Microbiologie pour l'Environnement (LCPME), UMR 7564, Université de Lorraine - CNRS, 405 rue de Vandœuvre, 54601 Villers-lès-Nancy, France*

(Dated: April 19, 2014)

Abstract

Powder and single crystal Raman spectra of the two most common phases of calcium carbonate are calculated with *ab initio* techniques (using a "hybrid" functional and a gaussian-type basis set) and measured both at 80 K and room temperature. Frequencies of the Raman modes are in very good agreement between calculations and experiments: the mean absolute deviation at 80 K is 4 and 8 cm^{-1} for calcite and aragonite, respectively. As regards intensities, the agreement is in general good, although the computed values overestimate the measured ones in many cases. The combined analysis permits to identify almost all the fundamental experimental Raman peaks of the two compounds, with the exception of either modes with zero computed intensity or modes overlapping with more intense peaks. Additional peaks have been identified in both calcite and aragonite, which have been assigned to ^{18}O satellite modes or overtones. The agreement between the computed and measured spectra is quite satisfactory; in particular, simulation permits to clearly distinguish between calcite and aragonite in the case of powder spectra, and among different polarization directions of each compound in the case of single crystal spectra.

Keywords: calcium carbonate, Polarized Raman spectra, single crystal, polycrystalline powder, Raman intensities, wavenumbers, quantum mechanical simulation, ab initio, CRYSTAL code

Corresponding authors:
cedric.carteret@univ-lorraine.fr (experiments);
marco.delapierre@unito.it (calculations).

I. INTRODUCTION

Anhydrous calcium carbonates can crystallize into three crystalline forms: calcite, aragonite and vaterite. The nucleation and crystal growth of calcium carbonate minerals is a process widely occurring in nature, mostly as a result of biomineralization.[1] In fact, calcium carbonate is the major constituent of coral reefs, shells, pearls and other biominerals, where it grows preferentially at ambient conditions due to the effect of organic templates[2]. This mineral also occurs in many other environments as deposition of hot springs, in stalactite and stalagmite cave formations[3]. From an industrial point of view, aside of the many applications as an additive, e.g. building materials, medicines, food, paper, plastics, printing inks,[4] it also represents a main problem in devices and desalination membranes due to the formation of scale.

While vaterite is a metastable polymorph that is mostly present in biological environments, calcite and aragonite are the main constituents of the majority of anhydrous calcium carbonate materials, and single crystals of good quality can be isolated for both these phases. Due to the complexity of vaterite, which forms extremely small single crystals having multiple structures and exhibiting chirality,[5–7] in this study we focus on aragonite and calcite. In particular, we present a comprehensive experimental and theoretical analysis of the Raman vibrational properties of these two phases, which includes the full classification of modes, wavenumbers and Raman intensities. Full range Raman spectra are here obtained from high quality single crystals, whose orientations were determined by X-ray diffraction, and polycrystalline powders. Accurate quantum mechanical *ab initio* simulations are also performed, capable of providing an extremely useful support in the processing of experimental measurements.

The first polarized Raman spectra of calcite and aragonite were measured by Couture[8]. This pioneering work was completed by Frech *et al.*[9] and Carteret *et al.*[10] for aragonite, and Porto *et al.*[11] for calcite, who discussed in detail the spectrum and polarization of Raman scattering in these calcium carbonate polymorphs. In recent times, Raman spectra have

also been used as an analytical tool by chemists and mineralogists to detect the different polymorphs.[12–16] However, a complete characterization of all spectral peaks, in terms of both frequency and intensity, is rarely performed; the attribution of spectral features to specific modes remains a hard task, too. Previous simulations on the vibrational properties of carbonates have mainly focused on methodological aspects,[17] on the effect of cation substitutions on the infrared spectra,[18] and on the role of the vibrational contributions to the relative stability of polymorphs.[19] Some of the present authors have recently presented an accurate study on the infrared and Raman properties of aragonite,[10] and a similar one had been devoted 8 years ago to calcite[20]; in both cases Raman intensities were not available. The recent implementation of the calculation of Raman intensities in the CRYSTAL code[21,22] permits the present study to achieve the main aims of reconstructing the full spectrum of the two compounds, and using the simulated data in the interpretation of the features of the experimental spectrum.

The paper is organized as follows: Section II is devoted to the description of the Raman experimental set up and of the examined samples. Section III presents the computational schemes adopted to perform the simulations. Results from theory and experiment are discussed and compared in Sections IV, V and VI. Section VII presents the main conclusions. Additional information is available as Supplementary Material[23]; Figures and Tables in this section are labelled with the "S" prefix.

II. EXPERIMENTAL DETAILS

The dimensions of the aragonite single crystal are about $5\times4\times2$ mm^3 along the a, b and c axes, respectively. The crystal was characterized by X-ray diffraction (XRD), proving a single $CaCO_3$ aragonite phase with lattice parameters $a = 4.9633$, $b = 7.9703$, $c = 5.7441$ Å, very close to the published refined structure[24]. The crystal was oriented by XRD, cut and polished to reveal (100), (010), (001) faces. The calcite single crystal, provided by MTI corporation, is a polished plate with dimensions $10\times10\times0.5$ mm^3 and (100) orientation. The lattice parameters are a= 4.989 and c= 17.062 Å.

Raman spectra were collected on a Jobin-Yvon T64000 spectrometer coupled to a N_2-cooled CCD detector and an Olympus optical microscope. Samples were excited by an argon ion laser beam at 514.5 nm using a Spectra Physics Stabilite 2017 laser. The laser beam was

focused on the sample via ×16 microscope objective (long working distance and 0.20 numerical aperture) with approximately 40 mW excitation power. The back-scattered Raman spectra were collected in confocal mode with a low numerical aperture objective to avoid optical artifacts. The Rayleigh scattering was removed by an edge filter and the Raman spectra were recorded between 90 and 1600 cm^{-1} with acquisition times of 5 minutes. The spectral resolution was around 1.3 cm^{-1}. The spectrometer was wavenumber calibrated using Raman Shift Frequency Standards (ASTM E 1840), so that the reported wavenumbers are accurate to less than 1 cm^{-1} of actual values. The Raman spectra were also intensity corrected for the effects of the beam splitter, the edge filter, the grating and the CCD detector response over the wavenumber range measured. The calibration was carried out with a calibrated QTH Source (Newport, Inc). This calibration permits quantitative comparison of spectral intensities obtained in different scattering orientations and allows measurements to be compared with theoretical predictions using a single scaling parameter.

The crystals were oriented along either a or b or c axes on the heating-cooling block of a Linkam THMS600 variable temperature cell deposited at the center of a rotation stage. The spectra were collected at 300 and 80 K. We made careful adjustment of the rotation stage to ensure the focused laser overlapping with the rotation stage center. The polarized Raman measurements were performed using a polarizer for both cross and parallel configurations (i.e., with respect to the incident laser polarization vector) and referred to for the (100) orientation as $x(zz)\overline{x}$ and $x(yz)\overline{x}$ respectively, according to Porto's notation[25]. The notation of the spectrum is described by four symbols, two inside parentheses and two outside. The inside symbols are, left to right, the polarizations of the incident and scattered beams, while the letters preceding and following the parentheses indicate the respective propagation directions of the incident and scattered beams. The x, y and z cartesian axes, according to the current laboratory reference, were selected as the a, b and c axes of the orthorhombic crystallographic structure, respectively. Extreme cares (orientation of the crystals, polarization of the incident laser source) were taken to avoid leakage of unexpected modes.

The Origin 8.5 program (OriginLab, Northampton, MA) was used for spectral data manipulation and curve fitting. The bands were fitted using a pseudo-Voigt line shape (mixed Gaussian and Lorentzian) with a polynomial baseline correction and were optimized by a non-linear least-squares fitting algorithm consisting of four adjustable parameters per band (position, FWHM, intensity, and percent Lorentzian character).

III. COMPUTATIONAL METHODS

Calculations were performed by using an all-electron Gaussian-type basis set, the hybrid Hartree-Fock/Density Functional B3LYP functional[26,27] and the 2014 release of the CRYSTAL code.[28,29] The chosen computational setup has been shown to reproduce structure and vibrational properties of ionic and semi-ionic compounds in excellent agreement with experimental data.[17,30–38] Supplementary calculations were performed by means of the Hartree-Fock Hamiltonian; corresponding data for single crystal calcite at 80 K are reported as Supplementary Information (Table S3). As regards intensities, critical qualitative aspects such as relative order remain unaltered when compared to B3LYP, even if quantitative agreement with experiment is slightly improved. On the other hand, three out of five frequencies show overestimations larger than 70 cm^{-1}.

A split-valence basis set of triple zeta quality with double set of d polarization functions was adopted. Oxygen, calcium and carbon are described by $(8s) - (411sp) - (1d1d)$, $(8s) - (6511sp) - (2d1d)$ and $(6s) - (311sp) - (1d1d)$ contractions, respectively, which have already been used in previous investigations of calcite (BSD in Ref. 20) and aragonite[10]. The complete basis sets and details on the computational parameters can be found on the CRYSTAL Web site[39], where input and output files used for the calculations are reported. Supplementary calculations were performed upon addition of a set of f polarization functions; the corresponding exponents were optimized in the present study, by taking calcite as the reference system. For sake of comparison, data obtained with this extended basis set for single crystals at 80 K are reported as Supplementary Information for both calcite and aragonite (Tables S4 and S5). Frequencies show slight variations in general; the only modes subject to larger changes are the ones below 100 cm^{-1} and above 1000 cm^{-1}, whose agreement with experiment worsens using the second basis set. More relevantly, intensities show only minor variations when adopting the second basis set; indeed, the corresponding statistical indices remain essentially unaltered.

The level of accuracy in evaluating the Coulomb and Hartree-Fock exchange series is controlled by five parameters[28] that have been set to 7 7 7 8 18. The threshold on the self-consistent field (SCF) energy was set to 10^{-10} Ha for both geometry optimization and construction of the Hessian. The reciprocal space was sampled according to a regular sublattice with shrinking factor[28] IS=6, corresponding to 32 (calcite) and 64 (aragonite) independent $\mathbf{k}$

vectors in the irreducible part of the Brillouin zone. The exchange-correlation contribution to the Fock matrix was evaluated by numerical integration over the unit cell volume. Radial and angular points of the grid are generated through Gauss-Legendre radial quadrature and Lebedev two-dimensional angular points distributions. In the present work, a pruned grid with 75 radial and 974 angular points was used (XLGRID keyword in the CRYSTAL14 manual[28]).

Structures were optimized by using the total energy analytical energy gradients with respect to atomic coordinates and unit cell parameters[40–42], within a quasi-Newton scheme combined with the BFGS algorithm for Hessian updating[43–46]. Convergence was checked on both gradient components and nuclear displacements, for which the default values[28] were chosen.

The calculation of the vibrational frequencies ν_0 at the Γ point was performed within the harmonic approximation. The key quantity is the matrix H of the second derivatives of the total energy V with respect to the atomic cartesian coordinates u, which was constructed by numerical differentiation of the analytical gradient vector v:

$$\begin{aligned} H_{\alpha i,\beta j} &= \frac{1}{2}\left[\frac{\partial^2 V}{\partial u_{\alpha i}\partial u_{\beta j}}\right]_0 = \frac{1}{2}\left[\frac{\partial v_{\alpha i}}{\partial u_{\beta j}}\right]_0 \\ &\approx \frac{1}{2}\frac{v_{\alpha i}(0,\cdots,u_{\beta j},0,\cdots) - v_{\alpha i}(0,\cdots,-u_{\beta j},0,\cdots)}{2u_{\beta j}} \end{aligned} \tag{1}$$

where greek and latin indices refer to atoms and atomic cartesian coordinates, respectively. Note that the calculated (optimized) equilibrium geometry is taken as a reference. The frequencies were then obtained as the eigenvectors of the mass-weighted Hessian matrix W at the Γ point:

$$W_{\alpha i,\beta j} = \frac{H_{\alpha i,\beta j}}{\sqrt{M_\alpha M_\beta}} \tag{2}$$

where M_α and M_β are the masses of atoms α and β. Once the Hessian matrix H is calculated, frequency shifts due to isotopic substitutions can be obtained at negligible computational cost (the expensive part of the calculation being the construction of the Hessian matrix, not its diagonalization), by changing the masses in Eq. (2). Further details on the calculation of vibrational frequencies can be found in Refs. 30,47,48.

Raman tensors were determined by means of a fully analytical approach[21,22] recently formulated by some of the present authors and implemented in the 2014 release of the CRYSTAL code. The formalism – that is an extension of the one developed in the context of infrared

intensities[49] – is based on the combination of energy gradients of the integrals[40,41] with a Coupled Perturbed Hartree-Fock/Kohn Sham (CPHF/KS) scheme[50,51] for the response of the density with respect to the electric field. The scheme is computationally efficient, since it avoids numerical differentiation with respect to either wave vectors or atomic coordinates. No perturbation equations for the atomic displacements need to be solved.

For an oriented single crystal, the Raman integrated intensity II associated with the ij component of the Raman tensor $\chi = \partial\alpha/\partial Q$ of the $n-th$ mode can be calculated as:[22,52]

$$II_n^{ij} \propto C \cdot V \cdot \left(\frac{\partial \alpha_n^{ij}}{\partial Q_n}\right)^2 \tag{3}$$

where V is the unit cell volume, α_n^{ij} is the polarizability component, Q_n is the normal mode coordinate and the prefactor C gives the dependence on temperature T and frequency of laser ν_L:[22,52]

$$C \sim (\nu_L - \nu_n)^4 \frac{1 + n_B(\nu_n)}{30\nu_n} \tag{4}$$

with the Bose occupancy factor being $1 + n_B(\nu_n) = [1 - \exp(-\hbar\nu_n/k_BT)]^{-1}$.

For a powder polycrystalline sample, the Raman integrated intensity of the $n-th$ mode can be obtained using the following formula:[52]

$$II_n^{tot} \propto C \cdot V \cdot [10G_n^{(0)} + 5G_n^{(1)} + 7G_n^{(2)}] \tag{5}$$

where the terms $G_n^{(k)}$ are the rotational invariants defined through:

$$G_n^{(0)} = \frac{1}{3}(\chi_n^{xx} + \chi_n^{yy} + \chi_n^{zz})^2 \tag{6}$$

$$G_n^{(1)} = \frac{1}{2}[(\chi_n^{xy} - \chi_n^{yx})^2 + (\chi_n^{xz} - \chi_n^{zx})^2 + (\chi_n^{yz} - \chi_n^{zy})^2] \tag{7}$$

$$G_n^{(2)} = \frac{1}{2}[(\chi_n^{xy}+\chi_n^{yx})^2+(\chi_n^{xz}+\chi_n^{zx})^2+(\chi_n^{yz}+\chi_n^{zy})^2]+\frac{1}{3}[(\chi_n^{xx}-\chi_n^{yy})^2+(\chi_n^{xx}-\chi_n^{zz})^2+(\chi_n^{yy}-\chi_n^{zz})^2] \tag{8}$$

Conventions for the Raman tensor[53–55] in the case of calcite (space group 167) and aragonite (s.g. 62) are reported in Table I. For each computed dataset, integrated intensities are normalized so that the value for a selected reference mode is set to 1000.

A graphical representation of the calculated Raman spectra $S(\nu)$ was obtained as a superposition of pseudo-Voigt functions, one for each mode:

$$S(\nu) = \sum_n [\eta_n \cdot L(\nu; \nu_{0,n}, II_n, \gamma_n) + (1 - \eta_n) \cdot G(\nu; \nu_{0,n}, II_n, \gamma_n)] \tag{9}$$

with:

$$L(\nu;\nu_{0,n},II_n,\gamma_n) = \frac{II_n}{\pi}\left[\frac{\gamma_n/2}{(\nu-\nu_{0,n})^2+\gamma_n^2/4}\right] \tag{10}$$

$$G(\nu;\nu_{0,n},II_n,\gamma_n) = 2\sqrt{\frac{\ln 2}{\pi}}\frac{II_n}{\gamma_n}\exp\left[-\frac{4\ln 2(\nu-\nu_{0,n})^2}{\gamma_n^2}\right] \tag{11}$$

where γ_n is the full width at half maximum of the $n-th$ mode peak and η_n is the Lorentz factor. L (the Lorentzian function) represents the response of the system itself to light scattering, while G (the Gaussian function) reproduces the response of the experimental apparatus. The combination of the two profiles, described by the γ and η parameters, is an almost unique feature of a given experiment. For γ, values obtained from the experimental spectra were adopted, for better readability of the figures; they are reported in the following along with measured frequencies and integrated intensities. For η, a unique average value of 0.7 has been adopted for all spectra. $S(\nu)$ curves were evaluated in the range of 50-1650 cm^{-1}, in steps of 0.5 cm^{-1}.

Frequencies and Raman integrated intensities (here both generically indicated as x) have been analyzed according to the following statistical indices (M is the number of data in the set): mean absolute difference between the calculated and the experimental values $\overline{|\Delta|} = M^{-1}\sum_{i=1}^{M}\left|x_i^{calc}-x_i^{exp}\right|$, mean difference $\overline{\Delta} = M^{-1}\sum_{i=1}^{M}\left(x_i^{calc}-x_i^{exp}\right)$, percentage mean absolute difference relative to the average of the experimental data $\overline{|\Delta|}\% = \overline{|\Delta|}/\overline{x}^{exp}\cdot 100 = \sum_{i=1}^{M}\left|x_i^{calc}-x_i^{exp}\right|/\sum_{i=1}^{M}x_i^{exp}\cdot 100$, maximum absolute difference $|\Delta|_{max} = \max_{i=1}^{M}\left|x_i^{calc}-x_i^{exp}\right|$.

Graphical animations of the normal modes are available at Refs. 56,57 so that the reader can directly interpret the "nature" of the mode (stretching, bending, rotation, translation, etc) in a simple and intuitive manner.

Manipulation and visualization of structures were performed with the Jmol 3D engine[58,59]. Data analysis was performed using the LibreOffice suite[60] and the Octave environment[61]. Graphs were realized with the Gnuplot utility[62].

IV. STRUCTURE AND SYMMETRY

The computed cell parameters for calcite are $a = 5.038$ and $c = 17.325$ Å, with a 1.0 and 1.5 % overestimation, respectively, compared with the experimental data. In the case of aragonite, calculations yield 5.008, 8.029 and 5.861 Å for the a, b and c axes, the differences

with respect to the experiment being +0.9, +0.7 and +2.0 %. These discrepancies are typical for the adopted functional (see, for example, Ref. 35).

The rhombohedral primitive cell of calcite contains 2 $CaCO_3$ formula units, for a total of 10 atoms; its 27 vibrational modes can be classified according to the irreducible representations of the $\overline{3}m$ point group as follows:

$$\Gamma_{total} = 1A_{1g} \oplus 2A_{1u} \oplus 3A_{2g} \oplus 3A_{2u} \oplus 4E_g \oplus 5E_u.$$

A_{1g} and E_g (double degenerate) modes are Raman active, A_{2u} and E_u (double degenerate) are IR active, A_{1u} and A_{2g} are spectroscopically inactive (silent modes).

The orthorhombic cell of aragonite contains 4 formula units, i.e. 20 atoms; its 57 vibrational modes can be classified according to the irreducible representations of the mmm point group as follows:

$$\Gamma_{total} = 9A_g \oplus 6A_u \oplus 6B_{1g} \oplus 8B_{1u} \oplus 9B_{2g} \oplus 5B_{2u} \oplus 6B_{3g} \oplus 8B_{3u}.$$

A_g, B_{1g}, B_{2g} and B_{3g} modes are Raman active, B_{1u}, B_{2u} and B_{3u} are IR active, A_u modes are silent.

V. POWDER POLYCRYSTALLINE DATA

Data for calcite and aragonite (at both 80 and 300 K) are reported in Tables II and III, respectively; the corresponding spectra are shown in Figures 1 and 2. Note that on the computational side the effect of temperature has been taken into account for the Raman tensors (i.e. for the integrated intensities), not for the vibrational frequencies. For each dataset Raman integrated intensities are renormalized so that the value for a selected reference peak is set to 1000. Calculations at present do not provide values for the peak widths γ, so only the experimental values are given in the Tables, for sake of reference. As calculated and experimental Raman frequencies for these compounds have already been compared and discussed in previous studies by some of the present authors[10,20], the present discussion will focus on Raman intensities and spectra. Finally, in the following and for sake of brevity integrated intensities will be simply referred to as intensities.

Calcite has 5 Raman active modes (Table II); for frequencies, the mean absolute and maximum deviations between calculation and experiment at 80 K are 4.2 and -10.6 cm^{-1}, respectively. If we have a look at the data for Raman intensities at 80 K, we note that all deviations

are positive, with a mean absolute value of 121 and a maximum value of 210 (corresponding to the E_g mode computed at 276.3 cm^{-1}). As the intensities span 4 orders of magnitude, it is worth defining a percentage mean absolute deviation to permit the comparison between different datasets; in this case it is equal to 49 %.

Aragonite has 30 active Raman modes (Table III). At 80 K 24 out of the 30 modes can be identified in the experimental spectrum. Of the 6 missing modes, 2 do have null computed intensity (modes 23 and 30), modes 14 and 20 are quite close to other peaks, whereas modes 9 and 12 sum up the two problems. The mean absolute deviation for frequencies is 8.0 cm^{-1}, whereas the maximum value is -25.3 cm^{-1}. As regards Raman intensities, the mean absolute deviation is 26; most discrepancies (19 out of 24) are positive, so that the mean deviation is positive and equal to 15. The percentage mean absolute deviation is 23 %; the maximum discrepancy is 82.

If we compare results at 300 K with those at 80 K, for both compounds we observe an improved agreement for frequencies, whereas deviations from experimental intensities increase. The fact that computed frequencies are closer to the room temperature rather than to the low temperature experimental values is likely related to the overestimation of the lattice parameters typical for the adopted Hamiltonian, which has been discussed in Section IV; such overestimation induces a general underestimation of the vibrational frequencies. Note also that, in the case of aragonite, at 300 K there are 2 more missing modes, due to superposition with more intense modes, which is in turn a consequence of the broadening of the peaks associated to the higher temperature.

As regards Raman intensities, a general overestimation of calculation with respect to experiment is observed, probably related to both uncertainties due to the experimental setup and approximations of the simulation. Concerning the latter aspect, basis set is the most likely source of discrepancy. For this study we adopted a high quality basis set for solid state calculations, whose accuracy in describing structure, vibrational frequencies and infrared intensities of minerals has been widely documented (see Section III). It is known from molecular calculations[63] that Raman intensities may require even richer basis sets, such as aug-cc-pVTZ or Sadlej pVTZ; however, development and assessment of these kinds of basis functions has so far not yet been addressed for solids.

Figures 1 and 2 show the Raman powder spectra for calcite and aragonite at both temperatures. Despite the discrepancies observed for the intensities, the relevant features of the

spectra are reproduced satisfactorily in all cases. It is worth comparing the powder spectra of calcite and aragonite (at 80 K for instance); as pointed out in Ref. 13, the two phases show the most relevant differences in the range 0-300 cm^{-1}: calcite has two peaks around 160 and 290 cm^{-1}, whereas aragonite has two intense peaks around 160 and 210 cm^{-1}. Notably, the two Figures show that the computational description of this frequency range permits a clear distinction between the two phases.

VI. SINGLE CRYSTAL DATA

In the following discussion, we will focus on the data at 80 K, to take advantage of the improved spectral resolution in the experiments. Data for calcite and aragonite are given in Tables IV and V, respectively; the corresponding spectra are shown in Figures 3 and 4. Single crystal data at 300 K are reported as Supplementary Information (Tables S1 and S2, Figures S1 and S2).

A. Calcite

Let us start discussing the 5 fundamental Raman modes of calcite (Table IV). Concerning the frequencies, as reasonably expected the mean absolute and maximum deviations are very close to the values found in the case of the powder data: 4.6 and -11.1 cm^{-1}, respectively. For single crystals, intensity data correspond to the elements of the Raman tensor of each mode (see also Table I). In this respect, single crystal data show a worse quality than the powder ones: the percentage mean absolute deviation is as large as 64 %. The mean absolute deviation is 57; 7 out of 9 discrepancies are positive, resulting in a mean deviation of 36. The maximum deviation is 172 and corresponds to the d^2 element of E_g mode computed at 276.3 cm^{-1}. Other two large deviations, 132 and -92, are found for the c^2 element of E_g mode at 711.0 cm^{-1} and for the b^2 element of the A_{1g} mode at 1089.1 cm^{-1}, respectively. We now comment on two spectral features that are found in the experimental spectra but not in the computed data. They are two minor, but yet visible, peaks at 1067.4 and 1749.8 cm^{-1}. These peaks are observed only in the spectra corresponding to XX and ZZ polarizations, which implies they must have a A_{1g} symmetry (to observe the peak at 1749.8 cm^{-1}, see Figure S3 in the Supplementary Information). As regards the first mode, at

1067.4 cm^{-1}, simulated isotopic substitution suggests this peak is the ^{18}O satellite mode of the very intense peak at 1087.1 cm^{-1} (isotopic shift 19.7 cm^{-1}). Graphical animation (`www.crystal.unito.it/prtfreq/jmol.html`) shows that the computed mode at 1089.1 cm^{-1} is the symmetric C-O stretching in the CO_3^{--} units. Upon substitution of a ^{16}O atom in a carbonate group with a ^{18}O atom, the carbonate units with "regular" ^{16}O atoms still stretch at this frequency; on the other hand, units bearing the ^{18}O isotope decouple from the others and stretch at 1068.3 cm^{-1}. The corresponding computed shift is 20.8 cm^{-1}, in excellent agreement with the experimental one.

The second additional peak is at 1749.8 cm^{-1}, well beyond the highest frequency of the fundamental modes, 1437.1 cm^{-1}. As proposed by Gillet *et al.*[64], this peak should be attributed to an overtone mode. By generating all the direct products of couples of fundamental modes yielding a mode with A_{1g} symmetry, two compatible combinations are found: 2×874.5 (A_{2u} symmetry, IR active) = 1749.1 cm^{-1} and 2×882.5 (A_{2g}, silent) = 1765.0 cm^{-1}. The corresponding deviations with respect to the experimental value are -0.7 cm^{-1} and 15.2 cm^{-1}. Even taking into account a possible anharmonic effect (not included in the calculations), the second value seems very far from the experiment, suggesting that the mode is more likely the overtone of the IR active mode computed at 874.5 cm^{-1}. Graphical animation (`www.crystal.unito.it/prtfreq/jmol.html`) shows that both modes are bendings of the CO_3^{--} units; in the former the two carbonates of the unit cell move in phase, in the latter they move in anti-phase.

B. Aragonite

Of the 30 fundamental Raman modes of aragonite (Table V), 28 can be identified in the single crystal measurement. Both missing modes (23 and 30) have 0 computed intensity. Compared with the powder experiment, 4 additional modes are identified: 9, 12, 14 and 20. As for calcite, the mean absolute and the maximum deviations are very close to the values found in the case of the powder data: 7.7 and -24.9 cm^{-1}.

A look at the intensities indicates that single crystal data for aragonite have a slightly larger percentage mean absolute deviation, 31 %, than in the powder case (23 %). The mean absolute deviation is 32. 36 out of 45 discrepancies are positive, giving a mean deviation of 26. The maximum deviation is 123, which corresponds to the e^2 element of the B_{2g} mode

computed at 182.5 cm^{-1}. Other 5 intensities have discrepancies larger than 100: A_g modes computed at 205.0 cm^{-1} (b^2 element) and 704.2 cm^{-1} (b^2 and c^2 elements), and B_{3g} modes at 167.6 and 701.2 cm^{-1} (f^2 element); also the e^2 element of the B_{2g} mode at 207.2 cm^{-1} shows a quite large deviation, 88.

Also in the case of aragonite we identify experimental peaks not belonging to the list of computed fundamental Raman modes: one at 1061.2 cm^{-1} (spectra with XX, YY, ZZ polarization; A_g symmetry) and one at 220.0 cm^{-1} (spectrum with XY polarization; B_{1g} symmetry). Similar to the case already discussed for calcite, the peak at 1061.2 cm^{-1} is attributed to a ^{18}O satellite mode of the intense peak at 1087.2 cm^{-1} (isotopic shift 26.0 cm^{-1}). Graphical animation (`www.crystal.unito.it/prtfreq/jmol.html`) indicates this mode as the symmetric C-O stretching in the CO_3^{--} units; the computed isotopic shift is 23 cm^{-1}, again in good agreement with the experimental one. This satellite mode has already been discussed in more detail by these authors[10]. As regards the additional mode at 220.0 cm^{-1}, a satisfactory assignation could not be found in the present study.

C. Spectra

Figures 3 and 4 show the Raman single crystal spectra for calcite and aragonite at 80 K. Zoomed views of the spectra for aragonite are available as Supplementary Information (Figure S4).

Despite the discrepancies described above for frequencies and, in particular, for intensities, the spectra for the various polarization directions are well characterized by the calculations, and clearly distinguished from each other. Indeed, for calcite the spectrum with $a^2 + c^2$ contributions, labeled as (ac) in Figure 3, has 4 peaks, the most intense being at 1089.1 cm^{-1}; the spectrum for b^2, (b) in the Figure, has only one peak at 1089.1 cm^{-1}; the spectrum for d^2, (d) in the Figure, has 4 peaks, too, the most intense being at 155.1 and 276.3 cm^{-1}.

Also in the case of aragonite, the computed spectra permit to clearly distinguish among different polarizations. There are three spectra involving modes with A_g symmetry; they feature the contributions from Raman tensors elements a^2, b^2 and c^2, and are labeled as (a), (b) and (c), respectively in Figure 4 (as well as in Figure S4 in the Supplementary Information). The three corresponding computed spectra all have the most intense peak at 1095.3 cm^{-1}. Spectrum (a) has two relatively intense peaks at 161.9 and 862.8 cm^{-1};

spectrum (b) has three features at 704.2, 205.0 and 280.2 cm^{-1}, whereas spectrum (c) has three features at 704.2, 148.7 and 161.9 cm^{-1}. The most intense peak of the spectrum (d) for d^2 is at 152.1 cm^{-1}, with other two features at 1463.9 and 97.4 cm^{-1}. Spectrum (e) for e^2 has the most intense peak at 207.2 cm^{-1} and another feature at 182.5 cm^{-1}. Finally, spectrum (f) for f^2 has the most intense peak at 701.2 cm^{-1}; as regards other relatively intense peaks, calculation indicates 167.6 and 271.4 cm^{-1}, at slight variance with the experiment (193.7 and 278.5 cm^{-1}).

VII. CONCLUSIONS

We have performed accurate *ab initio* calculations and experimental measurements of the Raman spectra of both calcite and aragonite phases of calcium carbonate.

The agreement between calculated and experimental frequencies is very good: the mean absolute deviation for calcite at 80 and 300 K is around 4 and 2 cm^{-1}, respectively; the same values for aragonite are 8 and 6 cm^{-1}. Calculation generally underestimates the experiment, which is likely related to the particular choice of the model Hamiltonian.

Calculated Raman intensity values, spanning a range of four orders of magnitude, agree reasonably well with the experimental data. Upon rescaling of the intensities to the most intense peak of each dataset, computed values generally overestimate measured ones. This issue is probably related to approximations and incertitudes from both computational and experimental sides, and calls for the development of superior quality basis sets for solid state calculations.

Overall, the agreement between the computed and measured spectra is quite satisfactory. In particular, simulation permits to clearly distinguish between calcite and aragonite in the case of powder spectra, as well as among different polarization directions of each compound in the case of single crystal spectra.

The combined analysis permits to identify and characterize almost all the fundamental Raman peaks of the two compounds, with the exception of either modes with zero computed intensity or modes overlapping with more intense peaks. Two additional peaks have been identified in both calcite and aragonite. In the former case, they correspond to ^{18}O satellite mode and to an overtone, respectively. In the latter case, one peak has been assigned to a ^{18}O satellite mode, too; the second peak remains at the moment unassigned.

As a final remark, previous papers by these authors have shown how powerful can be the interplay between theory and experiment in analyzing and interpreting the infrared spectra of minerals. The detailed discussion presented in the current paper strengthens this argument, extending the synergistic action to the field of Raman spectroscopy.

VIII. ACKNOWLEDGEMENTS

The authors acknowledge Compagnia di San Paolo for financial support (Progetti di Ricerca di Ateneo-Compagnia di San Paolo-2011-Linea 1A, progetto ORTO11RRT5). The authors also acknowledge the CINECA Award N. HP10BLSOR4-2012 for the availability of high performance computing resources and support. Improvements of the CRYSTAL code in its MPP version was made possible thanks to the PRACE proposal no. 2011050810 and ISCRA proposal NUCMOTDM - HP10AX8A2M.

s.g. 167									s.g. 62												
A_{1g}			$E_{g,1}$			$E_{g,2}$			A_g			B_{1g}			B_{2g}			B_{3g}		
a	·	·	c	·	·	·	$-c$	$-d$	a	·	·	·	d	·	·	·	e	·	·	·
·	a	·	·	$-c$	d	$-c$	·	·	·	b	·	d	·	·	·	·	·	·	·	f
·	·	b	·	d	·	$-d$	·	·	·	·	c	·	·	·	e	·	·	·	f	·

TABLE I: Convention for Raman tensor elements in the case of calcite (space group 167) and aragonite (s.g. 62)[53–55].

	Symmetry	ν					II_{tot}						$\gamma_{\exp}$	
			80 K		300 K		80 K			300 K			80 K	300 K
		calc.	exp.	Δ	exp.	Δ	calc.	exp.	Δ	calc.	exp.	Δ		
1	A_{1g}	1089.1	1087.1	*2.0*	1086.2	*2.9*	1000	1000		1000	1000		1.5	2.0
2	E_g	155.1	159.0	*-3.9*	154.9	*0.2*	239	184	*55*	425	295	*130*	2.6	7.1
3		276.3	286.9	*-10.6*	281.2	*-4.9*	843	633	*210*	1134	851	*283*	3.7	10.4
4		711.0	712.4	*-1.4*	712.4	*-1.4*	294	136	*158*	302	133	*169*	2.0	3.3
5		1433.3	1436.6	*-3.3*	1435.8	*-2.5*	96	34	*62*	95	33	*62*	2.4	4.5
$\overline{\lvert\Delta\rvert}$				*4.2*		*2.4*			*121*			*161*		
$\overline{\Delta}$				*-3.4*		*-1.1*			*121*			*161*		
$\overline{\lvert\Delta\rvert}$%									*49*			*49*		
$\lvert\Delta\rvert_{max}$				*10.6*		*4.9*			*210*			*283*		

TABLE II: Calculated and experimental Raman properties of powder polycrystalline calcite. In the calculations the temperature effect was taken into account for integrated intensities only. Frequencies ν and peak widths γ_{exp} are in cm^{-1}; for each temperature Raman integrated intensities were re-normalized so that value for A_{1g} mode at 1089.1 cm^{-1} is equal to 1000.

	Symmetry	ν					II_{tot}						γ_{exp}	
			80 K		300 K		80 K			300 K				
		calc.	exp.	Δ	exp.	Δ	calc.	exp.	Δ	calc.	exp.	Δ	80 K	300 K
1	A_g	148.7	144.4	*4.3*	142.9	*5.8*	31	27	*4*	57	60	*-3*	2.2	4.0
2		161.9	165.7	*-3.8*	162.2	*-0.3*	34	20	*14*	59	24	*35*	2.2	4.0
3		195.8	199.0	*-3.2*			28	5	*23*	44			3.0	
4		205.0	219.4	*-14.4*	214.7	*-9.7*	97	63	*34*	150	99	*51*	4.1	8.7
5		280.2	291.0	*-10.8*	283.6	*-3.4*	42	30	*12*	57	48	*9*	5.2	16.3
6		704.2	705.0	*-0.8*	706.1	*-1.9*	146	96	*50*	151	102	*49*	1.8	2.6
7		862.8	853.8	*9.0*	853.3	*9.5*	10	5	*5*	10	4	*6*	1.7	2.2
8		1095.3	1087.2	*8.1*	1085.3	*10.0*	1000	1000		1000	1000		1.5	1.9
9		1473.9					6			6				
10	B_{1g}	97.4	117.6	*-20.2*	113.5	*-16.1*	59	30	*29*	130	33	*97*	4.0	7.3
11		152.1	156.2	*-4.1*	153.0	*-0.9*	627	660	*-33*	1127	950	*177*	3.1	7.9
12		199.0					1			2				
13		213.4	226.5	*-13.1*	225.5	*-12.1*	25	9	*16*	38	9	*29*	4.5	10.0
14		705.5					11			11				
15		1463.9	1464.1	*-0.2*	1462.2	*1.7*	35	29	*6*	34	25	*9*	3.4	5.6
16	B_{2g}	182.5	183.9	*-1.4*	180.0	*2.5*	141	78	*63*	232	103	*129*	2.9	6.2
17		207.2	212.3	*-5.1*	206.3	*0.9*	339	370	*-31*	523	430	*93*	3.0	6.2
18		249.2	252.1	*-2.9*	248.3	*0.9*	82	68	*14*	115	52	*63*	5.6	9.7
19		260.7	266.1	*-5.4*	260.1	*0.6*	4	45	*-41*	5	45	*-40*	3.2	9.4
20		278.7					23			31				
21		714.6	716.7	*-2.1*	717.1	*-2.5*	7	10	*-3*	8	7	*1*	2.0	2.8
22		911.8	918.7	*-6.9*	918.2	*-6.4*	1	0	*1*	1	1	*0*	1.7	2.0
23		1091.6					0			0				
24		1591.8	1579.1	*12.7*	1573.9	*17.9*	31	11	*20*	31	10	*21*	4.6	7.8
25	B_{3g}	101.3	126.6	*-25.3*	125.0	*-23.7*	14	4	*10*	29	5	*24*	4.0	6.0
26		167.6	181.0	*-13.4*			94	11	*83*	160			3.7	
27		177.8	193.4	*-15.6*	190.7	*-12.9*	18	41	*-23*	29	80	*-51*	3.5	8.7
28		271.4	278.4	*-7.0*	272.0	*-0.6*	60	41	*19*	82	46	*36*	5.2	9.5
29		701.2	700.0	*1.2*	701.8	*-0.6*	138	64	*74*	142	75	*67*	1.6	2.2
30		1415.0					0			0				
$\overline{\lvert\Delta\rvert}$				*8.0*		*6.4*			*26*			*47*		
$\overline{\Delta}$				*-5.0*		*-1.9*			*15*			*38*		
$\overline{\lvert\Delta\rvert}$%									*23*			*32*		
$\lvert\Delta\rvert_{max}$				*25.3*		*23.7*			*82*			*177*		

TABLE III: Calculated and experimental Raman properties of powder polycrystalline aragonite. For each temperature Raman integrated intensities were re-normalized so that value for A_g mode at 1095.3 cm^{-1} is equal to 1000. See caption to Table II for more details.

		calc.	exp.	Δ	calc.	exp.	Δ	calc.	exp.	Δ	
	Symmetry		ν			a^2			b^2		$\gamma_{\rm exp}$
#	A_{1g}		1067.4			10			2		1.7
1		1089.1	1087.1	*2.0*	1000	1000		90	182	*-92*	1.4
#			1749.8			23			13		5.5
			ν			c^2			d^2		
2	E_g	155.1	159.6	*-4.5*	52	17	*35*	118	99	*19*	2.1
3		276.3	287.4	*-11.1*	73	58	*15*	526	354	*172*	3.2
4		711.0	712.6	*-1.6*	187	56	*131*	21	23	*-2*	1.8
5		1433.3	1437.1	*-3.8*	17	13	*4*	51	7	*44*	2.1
$\overline{\lvert\Delta\rvert}$				*4.6*						*57*	
$\overline{\Delta}$				*-3.8*						*36*	
$\overline{\lvert\Delta\rvert}$%										*64*	
$\lvert\Delta\rvert_{max}$				*11.1*						*172*	

TABLE IV: Calculated and experimental Raman properties of single crystal calcite at T = 80 K. Raman tensors were re-normalized so that the a^2 element of A_{1g} mode at 1089.1 cm^{-1} is equal to 1000. The symbols # indicate modes identified in the experiments with no correspondence in the calculations. See caption to Table II for more details.

		calc.	exp.	Δ	calc.	exp.	Δ	calc.	exp.	Δ	calc.	exp.	Δ	
	Symmetry		ν			a^2			b^2			c^2		γ_{exp}
1	A_g	148.7	144.7	*4.0*	3	1	*2*	1	2	*-1*	79	51	*28*	1.5
2		161.9	166.1	*-4.2*	49	11	*38*	6	0	*6*	45	44	*1*	1.7
3		195.8	199.2	*-3.4*	4	3	*1*	55	5	*50*	20	2	*18*	2.1
4		205.0	219.9	*-14.9*	5	1	*4*	234	120	*114*	43	27	*16*	2.9
5		280.2	291.5	*-11.3*	0	0	*0*	87	39	*48*	36	18	*18*	3.7
6		704.2	705.0	*-0.8*	1	1	*0*	217	104	*113*	216	99	*117*	1.6
7		862.8	854.0	*8.8*	24	5	*19*	0	2	*-2*	0	4	*-4*	1.8
#			1061.2			1			3			3		1.6
8		1095.3	1087.2	*8.1*	169	210	*-41*	977	980	*-3*	1000	1000		1.4
9		1473.9	1466.2	*7.7*	2	0	*2*	6	0	*6*	5	12	*-7*	1.8
			ν			d^2			e^2			f^2		
10	B_{1g}	97.4	117.6	*-20.2*	87	47	*40*							3.7
11		152.1	156.2	*-4.1*	931	918	*13*							2.8
12		199.0	211.7	*-12.7*	2	5	*-3*							3.5
#			220.0			3								3.0
13		213.4	227.0	*-13.6*	37	23	*14*							4.1
14		705.5	705.9	*-0.4*	16	14	*2*							1.6
15		1463.9	1464.1	*-0.2*	51	29	*22*							1.8
16	B_{2g}	182.5	184.6	*-2.1*				210	87	*123*				1.9
17		207.2	212.8	*-5.6*				503	415	*88*				2.2
18		249.2	252.5	*-3.3*				121	75	*46*				4.7
19		260.7	267.0	*-6.3*				6	53	*-47*				2.4
20		278.7	284.1	*-5.4*				34	6	*28*				5.0
21		714.6	716.9	*-2.3*				11	10	*1*				1.7
22		911.8	911.1	*0.7*				1	0	*1*				2.0
23		1091.6						0						
24		1591.8	1579.0	*12.8*				47	17	*30*				4.8
25	B_{3g}	101.3	126.2	*-24.9*							20	8	*12*	2.7
26		167.6	181.0	*-13.4*							139	17	*122*	2.3
27		177.8	193.7	*-15.9*							26	50	*-24*	2.3
28		271.4	278.5	*-7.1*							90	47	*43*	3.7
29		701.2	700.1	*1.1*							205	96	*109*	1.5
30		1415.0									0			
$\overline{\lvert\Delta\rvert}$				*7.7*									*32*	
$\overline{\Delta}$				*-4.6*									*26*	
$\overline{\lvert\Delta\rvert}$%													*31*	
$\lvert\Delta\rvert_{max}$				*24.9*									*123*	

TABLE V: Calculated and experimental Raman properties of single crystal aragonite at T = 80 K. Raman tensors were re-normalized so that the c^2 element of A_g mode at 1095.3 cm^{-1} is equal to 1000. The symbols # indicate modes identified in the experiments with no correspondence in the calculations. See caption to Table II for more details.

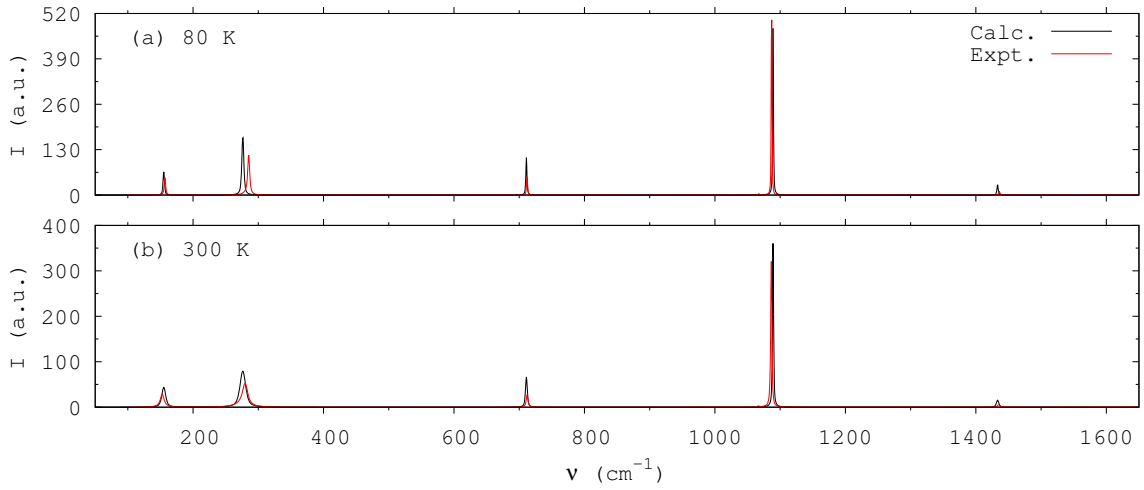

FIG. 1: Calculated and experimental Raman spectra of powder polycrystalline calcite. In the calculations the temperature effect was taken into account for integrated intensities only. For each temperature Raman integrated intensities were re-normalized so that the value for A_{1g} mode at 1089.1 cm^{-1} is equal to 1000.

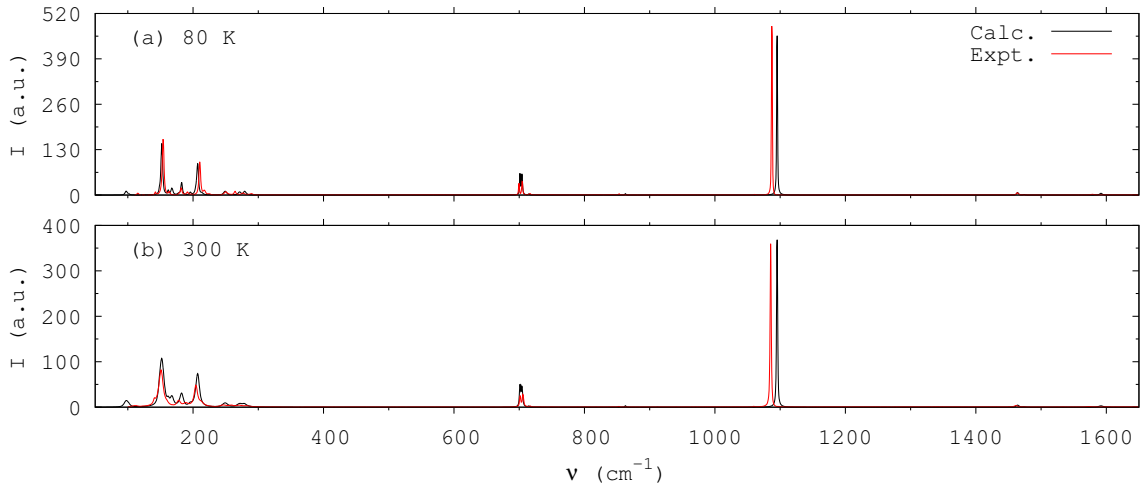

FIG. 2: Calculated and experimental Raman spectra of powder polycrystalline aragonite. In the calculations the temperature effect was taken into account for integrated intensities only. For each temperature Raman integrated intensities were re-normalized so that the value for A_g mode at 1095.3 cm^{-1} is equal to 1000.

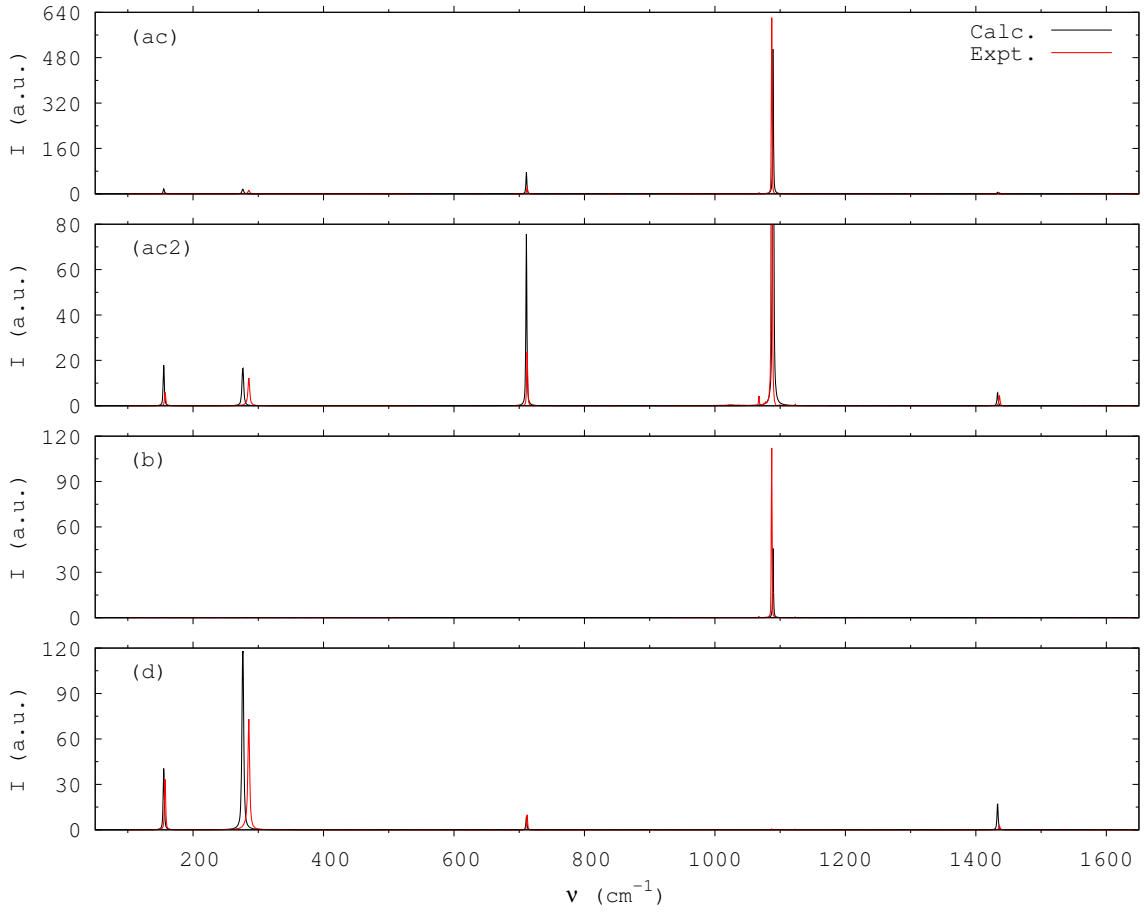

FIG. 3: Calculated and experimental Raman spectra of single crystal calcite at T = 80 K. In the calculations the temperature effect was taken into account for integrated intensities only. Raman integrated intensities were re-normalized so that the XX value for A_{1g} mode at 1089.1 cm^{-1} is equal to 1000. (ac) XX polarization, $a^2 + c^2$ contributions (A_{1g} plus E_g symmetries); (ac2) XX polarization, zoom on the c^2 contributions scale; (b) ZZ polarization, b^2 contributions (A_{1g}); (d) XZ polarization, d^2 contributions (E_g).

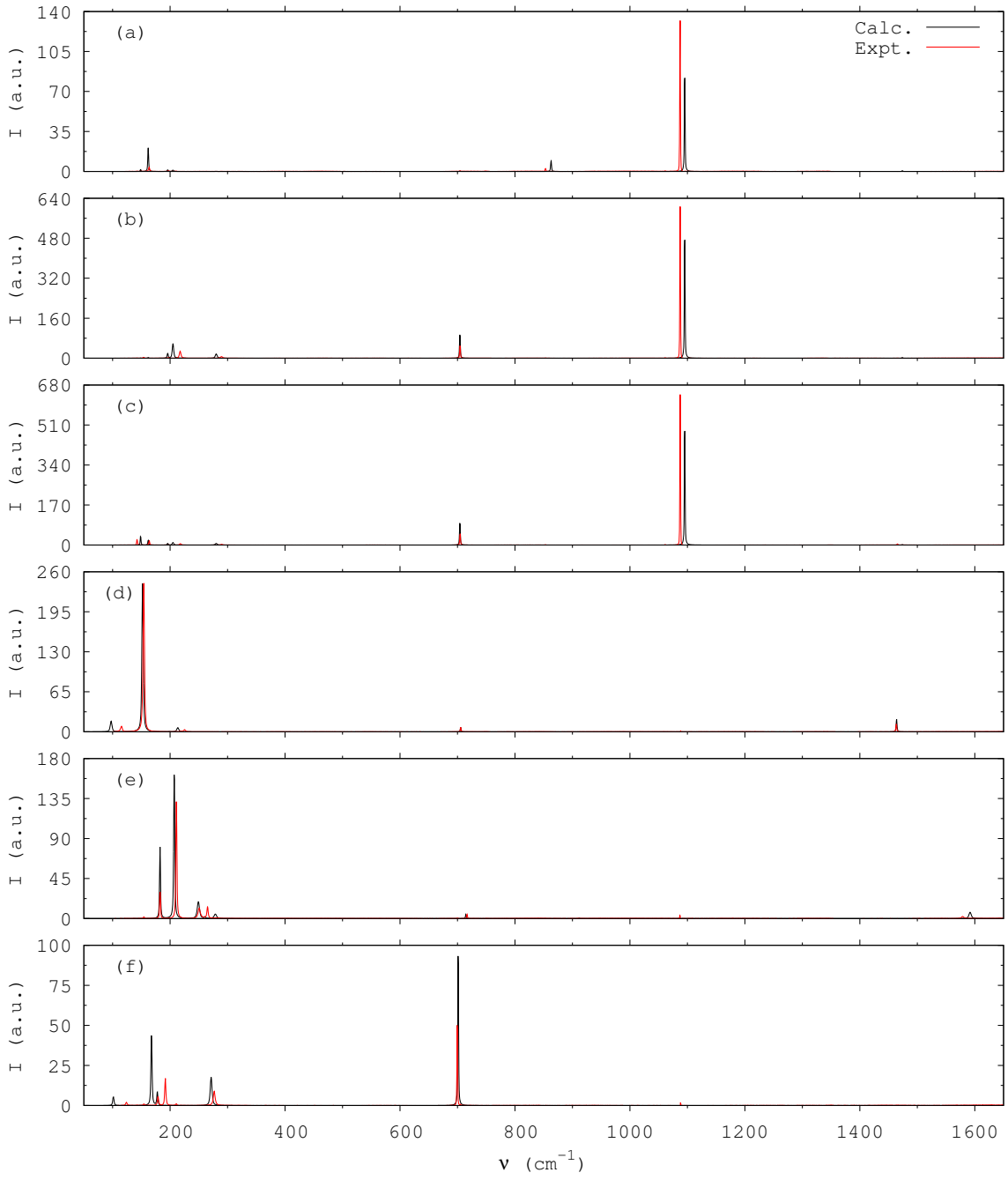

FIG. 4: Calculated and experimental Raman spectra of single crystal aragonite at T = 80 K. In the calculations the temperature effect was taken into account for integrated intensities only. Raman integrated intensities were re-normalized so that the ZZ value for A_g mode at 1095.3 cm^{-1} is equal to 1000. (a) XX polarization, a^2 contributions (A_g symmetry); (b) YY polarization, b^2 contributions (A_g); (c) ZZ polarization, c^2 contributions (A_g); (d) XY polarization, d^2 contributions (B_{1g}); (e) XZ polarization, e^2 contributions (B_{2g}); (f) YZ polarization, f^2 contributions (B_{3g}).

[1] W. A. Deer, R. A. Howie, and J. Zussman. *An introduction to the rock-forming minerals.* Longman Group, England, 1992.

[2] F. C. Meldrum. Calcium carbonate in biomineralisation and biomimetic chemistry. *Int. Mater. Rev.*, 48:187–224, 2003.

[3] J. W. Morse and F. T. Mackenzie. *Geochemistry of sedimentary carbonates.* Elsevier Science, 1990.

[4] J. G. Speight. *The Chemistry and Technology of Coal.* CRC Press Inc., 2012.

[5] R. Demichelis, P. Raiteri, J.D. Gale, and R. Dovesi. A new structural model for disorder in vaterite from first-principles calculations. *CrystEngComm*, 14:44–47, 2012.

[6] R. Demichelis, P. Raiteri, J.D. Gale, and R. Dovesi. The Multiple Structures of Vaterite. *Cryst. Growth Des.*, 13:2247–2251, 2013.

[7] L. Kabalah-Amitai, B. Mayzel, Y. Kauffmann, A.N. Fitch, L. Bloch, P.U.P.A. Gilbert, and B. Pokroy. Vaterite Crystals Contain Two Interspersed Crystal Structures. *Science*, 340:454–457, 2013.

[8] L. Couture. Vibrational spectra of single ionic crystals. *Ann. Physique*, 2:5–94, 1947.

[9] R. Frech, E. C. Wang, and J. B. Bates. The i.r. and Raman spectra of $CaCO_3$ (aragonite). *Spectrochim. Acta*, 36A:915–919, 1980.

[10] C. Carteret, M. De la Pierre, M. Dossot, F. Pascale, A. Erba, and R. Dovesi. The vibrational spectrum of CaCO3 aragonite: A combined experimental and quantum-mechanical investigation. *J. Chem. Phys.*, 138:014201, 2013.

[11] S. P. S. Porto, J. A. Giordmaine, and T. C. Damen. Depolarization of raman scattering in calcite. *Phys. Rev.*, 147:608–611, 1966.

[12] A. Dandeu, B. Humbert, C. Carteret, H. Muhr, E. Plasari, and J.-M. Bossoutrot. Raman spectroscopy - A powerful tool for the quantitative determination of the composition of polymorph mixtures: Application to CaCO3 polymorph mixtures. *Chem. Eng. Technol.*, 29:221–225, 2006.

[13] C. Carteret, A. Dandeu, S. Moussaoui, H. Muhr, B. Humbert, and E. Plasari. Polymorphism studied by Lattice Phonon Raman spectroscopy and Statistical Mixture Analysis Method. Aplli-cation to Calcium Carbonate Polymorphs during Batch Crystallization. *Cryst. Growth Des.*, 9:807–812, 2009.

[14] N. V. Vagenas, A. Gatsouli, and C. G. Kontoyannis. Quantitative analysis of synthetic calcium carbonate polymorphs using FT-IR spectroscopy. *Talanta*, 59:831–836, 2003.

[15] S. R. Dickinson and K. M. McGrath. Quantitative determination of binary and tertiary calcium carbonate mixtures using powder X-ray diffraction. *Analyst*, 126:1118–1121, 2001.

[16] C. G. Kontoyannis and N. V. Vagenas. Calcium carbonate phase analysis using XRD and FT-Raman spectroscopy. *Analyst*, 125:251–255, 2000.

[17] M. Prencipe, F. Pascale, C. M. Zicovich-Wilson, V. R. Saunders, R. Orlando, and R. Dovesi. The vibrational spectrum of calcite ($CaCO_3$): an ab initio quantum mechanical calculation. *Phys. Chem. Miner.*, 31:559–564, 2004.

[18] L. Valenzano, Y. Noël, R. Orlando, C. M. Zicovich-Wilson, M. Ferrero, and R. Dovesi. Ab initio vibrational spectra and dielectric properties of carbonates: magnesite, calcite and dolomite. *Theor. Chem. Acc.*, 117:991–1000, 2007.

[19] R. Demichelis, P. Raiteri, J. D. Gale, and R. Dovesi. Examining the accuracy of Density Functional Theory for predicting the thermodynamics of water incorporation into minerals: The hydrates of calcium carbonate. *J. Phys. Chem. C*, 117:17814–17823, 2013.

[20] L. Valenzano, F. J. Torres, K. Doll, F. Pascale, C. M. Zicovich-Wilson, and R. Dovesi. Ab Initio Study of the Vibrational Spectrum and Related Properties of Crystalline Compounds; the Case of $CaCO_3$ Calcite. *Z. Phys. Chem.*, 220:893–912, 2006.

[21] L. Maschio, B. Kirtman, M. Rérat, R. Orlando, and R. Dovesi. Ab initio analytical Raman intensities for periodic systems through a coupled perturbed Hartree-Fock/Kohn-Sham method in an atomic orbital basis. I. Theory. *J. Chem. Phys.*, 139:164101, 2013.

[22] L. Maschio, B. Kirtman, M. Rérat, R. Orlando, and R. Dovesi. Ab initio analytical Raman intensities for periodic systems through a coupled perturbed Hartree-Fock/Kohn-Sham method in an atomic orbital basis. II. Validation and comparison with experiments. *J. Chem. Phys.*, 139:164102, 2013.

[23] See Supplementary Material Document No._____ for additional data.

[24] E.N. Caspi, B. Pokroy, P.L. Lee, J.P. Quintana, and E. Zolotoyabko. On the structure of aragonite. *Acta Cryst B*, 61:129–132, 2005.

[25] T.C. Damen, S.P.S. Porto, and B. Tell. Raman effect in Zinc Oxide. *Phys. Rev.*, 142:570–574, 1966.

[26] A. D. Becke. Density-Functional Thermochemistry 3. The Role of Exact Echange. *J. Chem.*

Phys., 98:5648–5652, 1993.

[27] W. Koch and M. C. Holthausen. *A Chemist's Guide to Density Functional Theory.* Wiley-VCH Verlag GmbH, Weinheim, 2000.

[28] R. Dovesi, V. R. Saunders, C. Roetti, R. Orlando, C. M. Zicovich-Wilson, F. Pascale, B. Civalleri, K. Doll, N. M. Harrison, I. J. Bush, Ph. D'Arco, M. Llunell, M. Causà, and Y. Noël. *CRYSTAL14 User's Manual.* Università di Torino, Torino, 2014.

[29] R. Dovesi, R. Orlando, A. Erba, C.M. Zicovich-Wilson, B. Civalleri, S. Casassa, L. Maschio, M. Ferrabone, M. De La Pierre, Ph. D'Arco, Y. Noël, M. Causà, M. Rérat, and B. Kirtman. CRYSTAL14: A Program for the Ab Initio Investigation of Crystalline Solids. *Int. J. Quantum Chem.*, page DOI:10.1002/qua.24658, 2014.

[30] C. M. Zicovich-Wilson, F. Pascale, C. Roetti, V. R. Saunders R. Orlando, and R. Dovesi. The calculation of the vibration frequencies of α-quartz: the effect of Hamiltonian and basis set. *J. Comput. Chem.*, 25:1873–1881, 2004.

[31] F. Pascale, M. Catti, A. Damin, R. Orlando, V. R. Saunders, and R. Dovesi. Vibration frequencies of $Ca_3Fe_2Si_3O_{12}$ andradite. An *ab initio* study with the CRYSTAL code. *J. Phys. Chem. B*, 109:18522–18527, 2005.

[32] F. Pascale, C. M. Zicovich-Wilson, R. Orlando, C. Roetti, P. Ugliengo, and R. Dovesi. Vibration frequencies of $Mg_3Al_2Si_3O_{12}$ pyrope. An *ab initio* study with the CRYSTAL code. *J. Phys. Chem. B*, 109:6146–6152, 2005.

[33] R. Orlando, F. J. Torres, F. Pascale, P. Ugliengo, C. M. Zicovich-Wilson, and R. Dovesi. Vibrational Spectrum of Katoite $Ca_3Al_2[(OH)_4]_3$: A Periodic ab Initio Study. *J. Phys. Chem. B*, 110:692–701, 2006.

[34] R. Dovesi, L. Valenzano, F. Pascale, C.M. Zicovich-Wilson, and R. Orlando. Ab initio quantum-mechanical simulation of the Raman spectrum of grossular. *J. Raman Spectrosc.*, 40:416–418, 2009.

[35] R. Dovesi, M. De La Pierre, A. M. Ferrari, F. Pascale, L. Maschio, and C. M. Zicovich-Wilson. The IR vibrational properties of six members of the garnet family: a quantum mechanical ab initio study. *Am. Mineral.*, 96:1787–1798, 2011.

[36] R. Demichelis, H. Suto, Y. Noël, H. Sogawa, T. Naoi, C. Koike, H. Chihara, N. Shimobayashi, M. Ferrabone, and R. Dovesi. The infrared spectrum of ortho-enstatite from reflectance experiments and first-principle simulations. *Mon. Not. R. Astron. Soc.*, 420:147–154, 2012.

[37] Y. Noël, M. De La Pierre, L. Maschio, M. Rérat, C. M. Zicovich-Wilson, and R. Dovesi. Electronic Structure, Dielectric Properties and Infrared Vibrational Spectrum of Fayalite: An Ab Initio Simulation With an All-Electron Gaussian Basis Set and the B3LYP Functional. *Int. J. Quantum Chem.*, 112:2098–2108, 2012.

[38] M. De La Pierre, C. Carteret, R. Orlando, and R. Dovesi. Use of ab initio methods for the interpretation of the experimental IR reflectance spectra of crystalline compounds. *J. Comput. Chem.*, 34:1476–85, 2013.

[39] Input and output files.
`http://www.crystal.unito.it/supplement/raman-caco3/inpout.tar.gz`.

[40] K. Doll, V. R. Saunders, and N. M. Harrison. Analytical hartree-fock gradients for periodic systems. *Int. J. Quantum Chem.*, 82:1–13, 2001.

[41] K. Doll. Implementation of analytical hartree-fock gradients for periodic systems. *Comput. Phys. Comm.*, 137:74–88, 2001.

[42] B. Civalleri, Ph. D'Arco, R. Orlando, V. R. Saunders, and R. Dovesi. Hartree-Fock geometry optimisation of periodic systems with the CRYSTAL code. *Chem. Phys. Lett.*, 348:131–138, 2001.

[43] C. G. Broyden. The Convergence of a Class of Double-rank Minimization Algorithms 1. General Considerations. *J. I. Math. Appl.*, 6:76–90, 1970.

[44] R. Fletcher. A new approach to variable metric algorithms. *Comput. J.*, 13:317–322, 1970.

[45] D. Goldfarb. A Family of Variable-Metric Methods Derived by Variational Means. *Math. Comput.*, 24:23–26, 1970.

[46] D. F. Shanno. Conditioning of quasi-Newton methods for function minimization. *Math. Comput.*, 24:647–656, 1970.

[47] F. Pascale, C. M. Zicovich-Wilson, F. Liópez Gejo, B. Civalleri, R. Orlando, and R. Dovesi. The calculation of the vibrational frequencies of crystalline compounds and its implementation in the CRYSTAL code. *J. Comput. Chem.*, 25:888–897, 2004.

[48] C. M. Zicovich-Wilson, J. Torres, F. Pascale, L. Valenzano, R. Orlando, and R. Dovesi. The *ab initio* simulation of the IR spectra of Pyrope, Grossular and Andradite. *J. Comput. Chem.*, 29:2268–2278, 2008.

[49] L. Maschio, B. Kirtman, R. Orlando, and M. Rérat. Ab initio analytical infrared intensities for periodic systems through a coupled perturbed Hartree-Fock/Kohn-Sham method. *J. Chem.*

Phys., 137:204113, 2012.

[50] M. Ferrero, M. Rérat, B. Kirtman, and R. Dovesi. Calculation of first and second static hyperpolarizabilities of one- to three-dimensional periodic compounds. Implementation in the CRYSTAL code. *J. Chem. Phys.*, 129:244110, 2008.

[51] M. Ferrero, M. Rérat, R. Orlando, and R. Dovesi. The calculation of static polarizabilities of periodic compounds. The implementation in the CRYSTAL code for 1D, 2D and 3D systems. *J. Comput. Chem.*, 29:1450–1459, 2008.

[52] S.A. Prosandeev, U. Waghmare, I. Levin, and J. Maslar. First-order Raman spectra of AB'$_{1/2}$B"$_{1/2}$O$_3$ double perovskites. *Phys. Rev. B*, 71:214307, 2005.

[53] M. I. Aroyo, J. M. Perez-Mato, D. Orobengoa, E. Tasci, G. de la Flor, and A. Kirov. Crystallography online: Bilbao Crystallographic Server. *Bulg. Chem. Commun.*, 43:183–197, 2011.

[54] M. I. Aroyo, J. M. Perez-Mato, C. Capillas, E. Kroumova, S. Ivantchev, G. Madariaga, A. Kirov, and H. Wondratschek. Bilbao Crystallographic Server I: Databases and crystallographic computing programs. *Z. Krist.*, 221:15–27, 2006.

[55] M. I. Aroyo, A. Kirov, C. Capillas, J. M. Perez-Mato, and H. Wondratschek. Bilbao Crystallographic Server II: Representations of crystallographic point groups and space groups. *Acta Cryst. Sec. A*, 62:115–128, 2006.

[56] Calcite animations.
`http://www.crystal.unito.it/vibs/carbonates/`.

[57] Aragonite animations.
`http://www.crystal.unito.it/vibs/aragonite/`.

[58] Jmol 3d engine.
`http://jmol.sourceforge.net`.

[59] Jmoledit applet.
`http://www.theochem.unito.it/crystal_tuto/mssc2008_cd/tutorials/webvib/index.html`.

[60] Libreoffice suite.
`http://www.libreoffice.org`.

[61] Octave environment.
`http://www.gnu.org/software/octave`.

[62] Gnuplot utility.
`http://www.gnuplot.info`.

[63] C.A. Jiménez-Hoyos, B.G. Janesko, and G.E. Scuseria. Evaluation of range-separated hybrid density functionals for the prediction of vibrational frequencies, infrared intensities, and Raman activities. *Phys. Chem. Chem. Phys.*, 10:6621–6629, 2008.

[64] P. Gillet, P. McMillan, J. Schott, J. Badro, and A. Grzechnik. Thermodynamic properties and isotopic fractionation of calcite from vibrational spectroscopy of ^{18}O-substituted calcite. *Geochim. Cosmochim. Acta*, 60:3471–3485, 1996.